PbS/Polymer Nanocomposite Optical Materials with High Refractive Index

Changli Lü,[†,‡] Cheng Guan,[†] Yifei Liu,[†] Yuanrong Cheng,[†] and Bai Yang*[,†]

Key Lab of Supramolecular Structure & Materials, College of Chemistry, Jilin University, Changchun, 130012, P. R. China, and Institute of Chemistry, Northeast Normal University, Changchun, 130024, P. R. China

Received January 18, 2005. Revised Manuscript Received March 8, 2005

High refractive index nano-PbS/polymer composites were fabricated from reactive lead-containing precursors and polythiourethane (PTU) oligomer terminated with isocyanate group, followed by in situ gas/solid reaction. The lead-containing precursor with a chemical formula of $Pb(SCH_2CH_2OH)_2$ was synthesized in water phase at pH = 5−9 and exhibited an absorption at 317 nm in dimethyl sulfoxide (DMSO) in UV−vis spectra. PbS nanoparticles can be formed in DMSO after treatment with H_2S. TEM studies indicated that the PbS nanoparticles were smaller than 10 nm and aggregated seriously in DMSO. After the precursors were incorporated into PTU oligomer, the obtained composite films were treated with H_2S to obtain PbS nanoparticles/PTU nanocomposite films. TEM showed that the nanocomposites exhibited interesting phase behaviors depending on the precursor content in films. A uniform spherical aggregate of PbS nanoparticles (nanospheres) with a size smaller than 100 nm formed in the nanocomposite films below 26.3 wt % of lead-containing precursors. When the precursor content was larger than 59.3 wt %, the PbS nanoparticles about 3 nm dispersed uniformly in the whole polymer matrix. Ellipsometric measurement indicated that the precursors/PTU composite films before being treated with H_2S had a refractive index in the range 1.57−1.665 and after reaction with H_2S, the obtained PbS/PTU nanocomposite films had a higher refractive index in the range 1.57−2.06 with the varied content of precursors from 0 to 67 wt %.

Introduction

The composite and assembly of nanoparticles has been the research focus for scientists during the past decade.[1−5] The nanoparticles/polymer nanocomposites with functionality and high performance have attracted more attention due to their electrical, optical, magnetic, optoelectronic, and enhanced mechanical properties.[6−12] In particular, the nanocomposite optical materials with high refractive index, as the potential applications in filters, lenses, reflectors, optical waveguides, optical adhesives, and antireflection films, have been studied extensively.[6,7,13,14] Now incorporating inorganic domains into a polymer matrix is an effective way to fabricate high refractive index composite materials.[15−20] However, the size of inorganic domains must be below one-tenth of the wavelength of visible light (400−800 nm) in order to avoid Rayleigh scattering and obtain transparent polymer composites. So controlling the size of inorganic domains in the nanometer regime is very important. Recently, a series of TiO_2-polymer hybrid materials have been prepared through a sol−gel process.[16,17,21−23] The titania domains in these hybrids can be easily controlled in nanoscale. But the titania domain in hybrid materials obtained by this method is amorphous and its refractive index is relatively low (about 2.0). The refractive index of these hybrid materials obtained by this method is usually less than 1.85. Some semiconductor nanoparticles of metal sulfide have a high refractive index and can be introduced into polymer matrix to prepare high

* Corresponding author. E-mail: byangchem@jlu.edu.cn. Fax: +86-431-5193423.
† Jilin University
‡ Northeast Normal University.

(1) Komarneni, S.; Parker, J. C.; Thomas, G. J. *Nanophase and nanocomposite. materials*; Materials Research Society: Pittsburgh, PA, 1993.
(2) Pomogailo, A. D. *Russ. Chem. Rev.* **2000**, *69*, 53.
(3) Fendler, J. H. *Chem. Mater.* **2001**, *13*, 3196.
(4) Decher, G. *Science* **1997**, *277*, 1232.
(5) Caruso, F.; Caruso, R. A.; Möhwald, H. *Science* **1998**, *282*, 1111.
(6) Beecroft, L. L.; Ober, C. K. *Chem. Mater.* **1997**, *9*, 1302.
(7) Caseri, W. *Macromol. Rapid Commun.* **2000**, *21*, 705.
(8) Zhang, H.; Cui, Z. C.; Wang, Y.; Zhang, K.; Ji, X. L.; Lü, C. L.; Yang B.; Gao, M. Y. *Adv. Mater.* **2003**, *15*, 777.
(9) Kanatzidis, M. G.; Wu, C. *J. Am. Chem. Soc.* **1989**, *111*, 4139.
(10) Alivistatos, A. P. *J. Phys. Chem.* **1996**, *100*, 13226.
(11) Takafuji, M.; Ide, S.; Ihara, H.; Xu, Z. *Chem. Mater.* **2004**, *16*, 1977.
(12) Müh, E.; Frey, H.; Klee, J. E.; Mülhaupt, R. *Adv. Funct. Mater.* **2001**, *11*, 425.
(13) Papadimitrakopoulos, F.; Wisniecki, P.; Bhagwagar, D. E. *Chem. Mater.* **1997**, *9*, 2928.
(14) Yoshida, M.; Prasad, P. N. *Chem. Mater.* **1996**, *8*, 235.
(15) Olshavsky, M. A.; Allcock, H. R. *Macromolecules* **1995**, *28*, 6188.
(16) Wang, B.; Wilkes, G. L.; Hedrick, J. C.; Liptak, S. C.; Mcgrath, J. E. *Macromolecules* **1991**, *24*, 3449.
(17) Lee, L. H.; Chen, W. C. *Chem. Mater.* **2001**, *13*, 1137.
(18) Zimmermann, L.; Weibel, M.; Caseri, W.; Suter, U. W. *J. Mater. Res.* **1993**, *8*, 1742.
(19) Lü, C. L.; Cui, Z. C.; Li, Z.; Yang, B.; Shen, J. *J. Mater. Chem.* **2003**, *13*, 526.
(20) Lü, C. L.; Cui, Z. C.; Wang, Y.; Li, Z.; Guan, C.; Yang, B.; Shen, J. C. *J. Mater. Chem.* **2003**, *13*, 2189.
(21) Lü, C. L.; Cui, Z. C.; Guan, C.; Guan, J. Q.; Yang, B.; Shen, J. C. *Macromol. Mater. Eng.* **2003**, *288*, 717.
(22) Nussbaumer, R. J.; Caseri, W. R.; Smith, P.; Tervoort, T. *Macromol. Mater. Eng.* **2003**, *288*, 44.
(23) Chang, C. C.; Chen, W. C. *J. Polym. Sci., Part A: Polym. Chem.* **2001**, *39*, 3419.

10.1021/cm050113n CCC: $30.25
Published on Web 04/09/2005

refractive index nanocomposites. For example, the nanoparticles of lead sulfide[18,24,25] and iron sulfide[26] have been introduced into poly(ethylene oxide) or gelatin to produce nanocomposites with higher refractive index. However, the polymer matrixes used in these studies are water-soluble polymers and there is no chemical bonding between the nanoparticles and polymer matrixes. So the application of such composite materials is restrained in many fields, where the materials with water insolubility, good thermal stability, and mechanical properties are needed. With these drawbacks in view, the pre-made nano-ZnS particles surface-capped with functionalized thiols have been used for fabrication of polymer nanocomposite films with high refractive index in our laboratory recently.[19,20] This method provides full synthetic control over both the nanoparticles and matrix. In addition, these nanocomposites exhibited good thermal stability and excellent optical properties.

In this paper, we present a novel method for in situ incorporation of PbS nanoparticles into water-insoluble polymer matrix to fabricate higher refractive index nanocomposites. First, a lead-containing precursor with functional hydroxyl groups was synthesized from mercaptoethanol (ME) and lead nitrate in water phase at pH = 5−9. Then the lead-containing precursors as building blocks of polymer networks were introduced into polythiourethane (PTU) matrix via polyaddition of hydroxyl groups in ME molecule in precursors with isocyanate groups of PTU oligomer. A transparent PbS/PTU nanocomposite film can be easily obtained through exposing the precursors/PTU composites to H_2S gas. The lead-containing precursors and the resulting nanocomposite films were characterized by UV−vis spectra, FTIR, TEM, and TGA. The refractive indices of the resulted films were measured at the wavelength of 632.8 nm by an ellipsometer.

Experimental Section

Materials. Lead nitrate, 2-mercaptoethanol (ME), sodium hydroxide, $Na_2S{\cdot}9H_2O$, isophorone diisocyanate (IPDI), and dibutyltin diaurate (DBTL) were all of analytical-grade reagents and were used without further purification. 2,2′-Dimercaptoethyl sulfide (MES) was synthesized as reported previously.[27,28] Toluene and dimethyl sulfoxide (DMSO) were distilled from molecular sieves and anhydrous magnesium sulfate, respectively.

Synthesis of Lead-Containing Precursor. Two grams of lead nitrate was dissolved in 40 mL of water and under N_2 flow 1.0 mL of mercaptoethanol was put into this stirred solution on an ice bath. After the mixture was stirred for 40 min, the solution became yellow in color. Then the pH of the resulting solution was adjusted between 1.4 and 9.0 by adding dropwise 1 M sodium hydroxide solution. Finally, the solids were filtered and washed several times with excess amounts of water, followed with acetone, and the resultant powder was collected and dried under vacuum.

Formation of PbS Nanoparticles in DMSO Solution. Lead-containing precursor was dissolved in DMSO to form a 5×10^{-4} M solution of lead-containing precursor. Excess amounts of H_2S gas were introduced into the above DMSO solution, and the solution became brown in color, indicating that the PbS nanoparticles were formed in DMSO solution.

Synthesis of Isocyanate Group Terminated Polythiourethane (PTU) Oligomer. MES (7.7 g, 0.05 mol) and IPDI (16.7 g, 0.075 mol) were dissolved in 50 mL of dry toluene. Then, 0.05 g of DBTL was added to catalyze the reaction. This solution was stirred under nitrogen flow at 80 °C for 10 h. A 61 wt % solution of PTU oligomer in toluene was obtained as a colorless and transparent viscous liquid by removing most of the toluene under reduced pressure. FT-IR (cm^{-1}): 3290 [ν (NH)], 2268 [ν (NCO)], 1667 [ν (COS)], 1530 [ν (NH)], 1254 [δ (NH)].

Preparation of PbS/Polythiourethane Nanocomposite Films. Lead-containing precursors and PTU oligomer of desired weight ratio were dissolved in DMSO, respectively. Then, the above two solutions were mixed completely and the mixture solution was dip-coated on pretreated silicon wafers. The coated films were heated under vacuum at 70 °C for 5 h, 100 °C for 1 h, and 120 °C for 1 h. The resulting films were exposed to excess H_2S gas for 24 h in a closed vessel and the PbS/polythiourethane nanocomposites with different contents of PbS particles were obtained.

Characterization. FTIR spectra were recorded on a Nicolet AVATAR360 FTIR spectrometer. ^1H NMR spectra were obtained from an AVANCE 500 MHz Bruker spectrometer in d_6-DMSO solution. UV−vis absorption spectra were recorded on a Shimadzu 3100 UV−vis−NIR spectrometer in the range 200−800 nm. Elemental analysis (EA) was performed by a Perkin-Elmer 2400 series II analyzer. Thermogravimetric analysis (TGA) was performed on a Perkin-Elmer TGA7 at a heating rate of 10 °C min^{-1} under nitrogen flow from 50 to 700 °C. Transmission electron microscopy (TEM) was carried out using a JEOL-2021 microscope. Nanocomposite samples with a thickness of about 70 nm on copper grid for TEM were prepared by ultracut microtome. The refractive indices of the nanocomposite films at the wavelength of 632.8 nm were measured on an AUEL-III auto-laser ellipsometer equipped with a He−Ne laser (λ = 632.8 nm).

Results and Discussion

Synthesis and Characterization of Lead-Containing Precursors. Because mercapto group has a strong coordination to the lead ions, a strong lead-containing complex (lead thiolates) can be easily formed in the presence of thiol (RSH). Thiolates of metals containing Pb, Cd, or Zn generally were prepared in hot organic solvent such as ethanol and tetrahydrofuran (THF), through the reaction of metallic acetate or nitrate with thiols.[29−34] All of the lead thiolates were synthesized in hot ethanol in the previous reports, and these thiolates were poorly soluble in organic solvent. However, there are a few reports about the preparation of lead thiolates in aqueous solution from thiols and lead salt.[35] In addition, in the previous studies only the type and formation condition (concentration and pH) of thiolates were investigated and

(24) Webel, W.; Caseri, W.; Suter, U. W.; Kiss, H.; Wehrli, E. *Polym. Adv. Technol.* **1991**, *2*, 75.
(25) Kypriandou-Leodidou, T.; Caseri, W.; Suter, U. W. *J. Phys. Chem.* **1994**, *98*, 8992.
(26) Kypriandou-Leodidou, T.; Althaus, H. J.; Wyser, Y.; Vetter, D.; Büchler, M.; Caseri, W.; Suter, U. W. *J. Mater. Res.* **1997**, *12*, 2198.
(27) Reid, E. E. *Organic Chemistry of Bivalent Sulfur*; Chemical Publishing Co.: New York, 1985; Vol. 1, issue 1, p 33.
(28) Gao, C.; Yang, B.; Shen, J. *J. Appl. Polym. Sci.* **2000**, *75*, 1474.
(29) Wang, Y.; Herron, N. *Chem. Phys. Lett.* **1992**, *200*, 71.
(30) Boudjouk, P.; Jarabek, B. R.; Simonson, D. L.; Seidler, D. J.; Grier, D. G.; McCarthy, G. J.; Keller, L. P. *Chem. Mater.* **1998**, *10*, 2358.
(31) Shaw, R. A.; Woods, M. *J. Chem. Soc.* **1971**, 1570.
(32) Haberkorn, R. A.; Que, L.; Gillum, W. O.; Holm, R. H.; Liu, C. S.; Lord, R. C. *Inorg. Chem.* **1976**, *15*, 2408.
(33) Arsenault, J. J. I.; Dean, P. A. W. *Can. J. Chem.* **1983**, *61*, 1516.
(34) Olshavsky, M. A.; Allcock, H. R. *Chem. Mater.* **1997**, *9*, 1367.
(35) Nenadović, M. T.; Comor, M. I.; Vasić, V.; Mićić, O. I. *J. Phys. Chem.* **1990**, *94*, 6390.

Table 1. Elemental Analysis for Lead-Containing Precursors at Different pHs

element	pH = 1.4	pH = 3	pH = 4.5	pH = 5	pH = 6.28	pH = 7	pH = 8.5−9	calc.[a]
C	7.08	7.10	10.28	13.76	13.39	13.35	13.34	13.30
H	1.40	1.36	1.96	2.71	2.70	2.74	2.69	2.79
N	3.67	3.66	1.62					
S	8.92	9.12	12.39	16.87	17.85	17.71	17.68	17.73

[a] Theoretical calculation values of different elements for the lead-containing precursor with a chemical formula of $Pb(SCH_2CH_2OH)_2$.

no pure thiolates were obtained. In the present work, we synthesized a series of different lead thiolates in aqueous phase at pH = 1.4−9 and the resulting lead thiolates exhibited good solubility in DMSO (the gray lead oxide was formed at pH > 9). Through elemental analysis, we determined the composition of lead thiolates at different pH (Table 1). The results show that the S content in thiolates gradually increases with the increasing pH and becomes a constant at pH = 5−9. The relative molar ratio of C, H, and S element was calculated to be 2:5:1 at pH = 5−9. This result indicates that only one mononuclear complexes (the chemical structural formula is $Pb(SCH_2CH_2OH)_2$, mp: 99−104 °C) are formed at pH > 5, while a mixture of mononuclear and polynuclear lead thiolates(complexes) may be formed at pH < 5. There is a sharp contrast between our results and previous work,[35] in which complexes of 3-mercapto-1,2-propanediol and lead acetate were investigated. To determine the detailed structure of lead thiolates, attempts to obtain the single crystal of lead thiolates were unsuccessful. So the steric structure of the lead thiolate [$Pb(SCH_2CH_2OH)_2$] is unknown at present. In the following discussion, we will mainly focus on the lead thiolate [($Pb(SCH_2CH_2OH)_2$] formed at pH = 5−9 and the nanocomposite from the lead thiolate as lead-containing precursors.

Figure 1 shows the FTIR spectrum of lead-containing precursors obtained at pH = 5−9. The absorption peak of S−H vibration for ME at 2545 cm^{-1} is not observed in the IR spectrum, indicating that the mercapto groups of ME molecules were bound to the lead ions to form a complex. The peaks at 3211 and 3088 cm^{-1} are assigned to the characteristic vibration of the hydroxyl groups, and the two absorption peaks appear below 3500 cm^{-1} in the IR spectrum. This is probably because of intramolecular hydrogen bond and steric hindrance effect, which makes the vibration of hydroxyl groups move to lower wavenumber and forms two different vibration fashions. Another probable reason is from the coordination of partly hydroxyl groups with the lead ions. C−O stretching and −OH bending vibrations appear at 1221−1015 cm^{-1} and 1275−1360 cm^{-1}, respectively. The peaks assigned to stretching and in-plane bending vibrations of methylene groups are observed at 2873−2925 cm^{-1} and 1466 cm^{-1}. The above analyses indicate that the precursors are a metal organic complex formed by lead ions and ME. However, the characteristic vibration of the Pb−S bond cannot be detected in the FTIR spectrum.

The ^1H NMR spectra of lead-containing precursors and mercaptoethanol (ME) in DMSO are shown in Figure 2. It can be seen that the lead-containing precursor exhibits three groups of different chemical shifts [3.49 ppm (t, 4H), 3.68 ppm (t, 4H) and 5.28 ppm (s, 2H)] and the mercaptoethanol (ME) exhibits four groups of chemical shifts [2.12 ppm (t, 1H), 2.53 ppm (q, 2H), 3.48 ppm (t, 2H), 4.88 ppm (s, 1H)]. The peak of mercapto group (2.12 ppm) on ME disappears in the ^1H NMR spectrum of lead-containing precursors, indicating the formation of the complex from lead ions and ME. The peaks of hydroxyl groups (5.28 ppm) and methylene groups (3.49 and 3.68 ppm) in lead-containning precursors appear at higher chemical shifts compared with that of ME due to the change of chemical circumstance. In addition, the peak of hydroxyl groups of lead-containing precursors at 5.28 ppm (4.88 ppm for ME) exhibits a single peak due to the strong attraction electron effect of oxide atom and the hydrogen bond as well as the proton exchange.

The UV−vis absorption spectrum of lead-containing precursors (5×10^{-4}M) in DMSO is shown in Figure 5a(c). There is a maximum absorption at 317 nm in the absorption spectrum. Because the absorption of thiolate ligand (ME) is below 250 nm, the absorption at 317 nm is ascribed to the

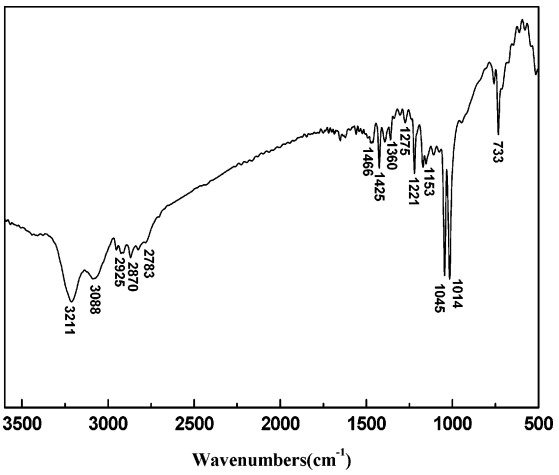

Figure 1. FTIR spectrum of lead-containing precursor obtained at pH = 5−9.

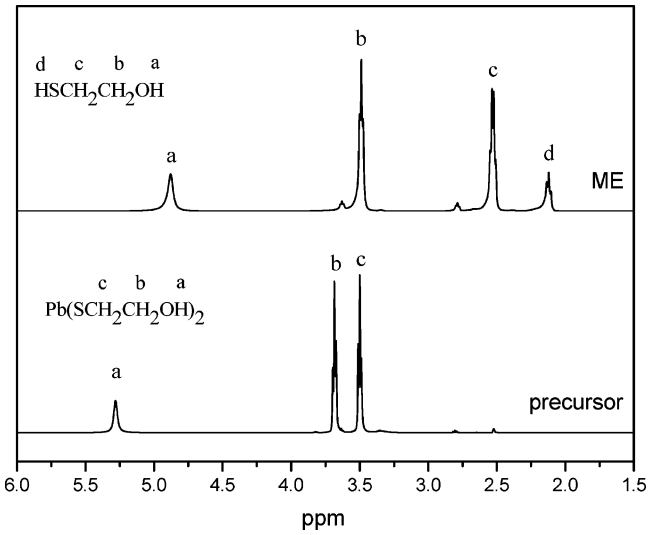

Figure 2. ^1H NMR spectra of mercaptoethanol (ME) and lead-containing precursors in DMSO-d_6.

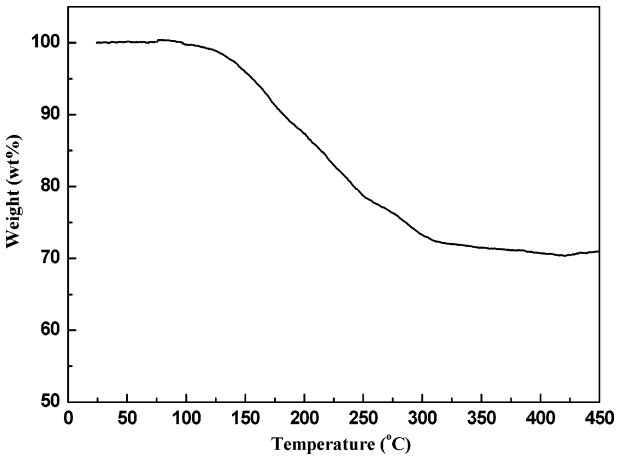

Figure 3. TGA curve of lead-containing precursors.

excited transition of precursors.[36] This absorption value is in agreement with the previous report for similar complexes obtained at pH = 7 or 8.[35]

TGA curve of lead-containing precursors shows the precursors begin to decompose at 130 °C and completely form bulk PbS solid at 330 °C (Figure 3). The final char yield of precursors (71 wt %) is slightly higher than theoretical calculation value (66 wt %). This is probably attributed to the organic moiety trapped in the inorganic solid matrix or residual carbons.

Formation of PbS Nanoparticles from Lead-Containing Precursors in DMSO. We synthesized PbS nanoparticles in DMSO through reaction of lead-containing precursors with H_2S gas. However, the poor stability of the formed PbS particles in DMSO was observed, especially for the high concentration of precursors in DMSO solution. The corresponding TEM image and selected area electron diffraction patterns (inset) of the PbS nanoparticles is illustrated in Figure 4. The PbS particles formed in DMSO seriously aggregate; however, the congeries is composed of PbS nanoparticles less than 10 nm in diameter. Selected area electron diffraction pattern (SAED) shows that the PbS particles have a cubic rock salt structure.

Preparation and Characterization of PbS/PTU Nanocomposites. The lead-containing precursors were introduced into the isocyanate-capped PTU oligomer, followed by dip-coating and heat-curing process to form lead-containing polymer films. Then, the films were exposed to H_2S gas in order to in situ generate PbS nanoparticles in polymer matrix. The films rapidly turn from light yellow to brown yellow or brown depending on the content of lead-containing precursors, indicating the formation of PbS nanoparticles/polymer nanocomposites.

Figure 5 shows the UV−vis absorption spectra of the precursors/PTU composites before and after reaction with H_2S gas, respectively. It can be seen that, after reaction of the different contents of precursors with the PTU oligomers, there are absorption peaks at 357 nm in absorption spectra (Figure 5a). Compared with the maximum absorption of precursors at 317 nm in DMSO, the absorption peaks of

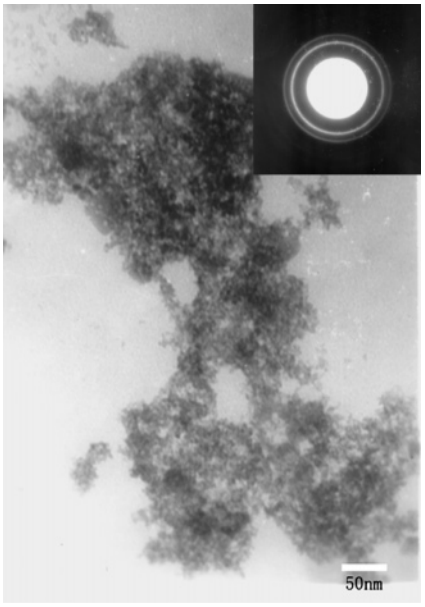

Figure 4. TEM image and selected area electron diffraction pattern (inset) of PbS nanoparticles.

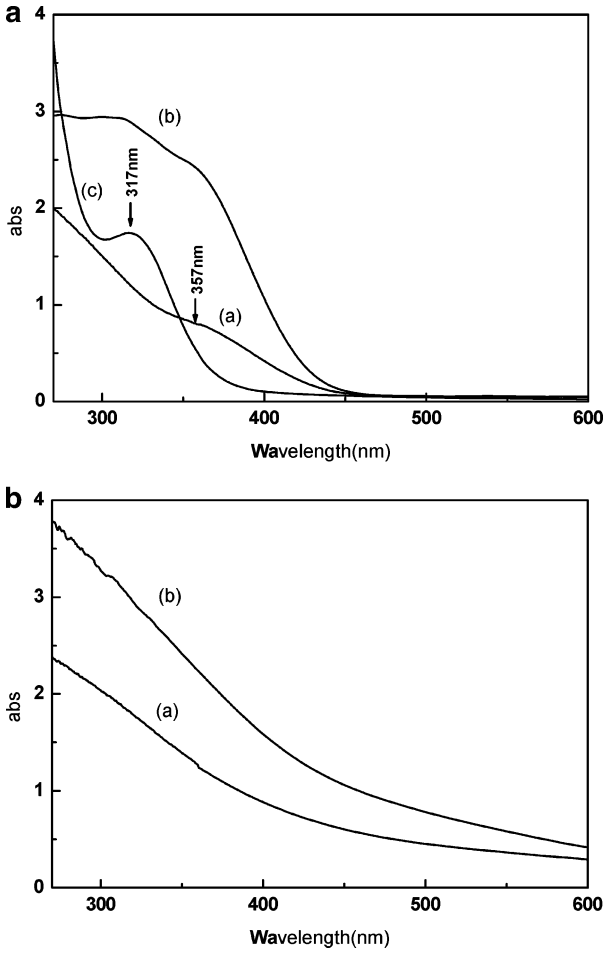

Figure 5. a. UV−vis absorption spectra of precursors/PTU films before treatment with H_2S gas: (a) 26.3 wt % precursors; (b) 59.3 wt % precursors; (c) lead-containing precursors in DMSO ($M = 5 \times 10^{-4}$ M). b. UV−vis absorption spectra of precursors/PTU films after treatment with H_2S gas (a) 26.3 wt %; (b) 59.3 wt % precursors.

precursors/PTU composite exhibit a red shift. This is probably due to the interaction between precursors and polymers after the precursors become the composing segments of polymer composites and are immobilized into the

(36) Vossmeyer, T.; Reck, G.; Katsikas, L.; Haupt, E. T. K.; Schulz, B.; Weller, H. *Science* **1995**, *267*, 1476.

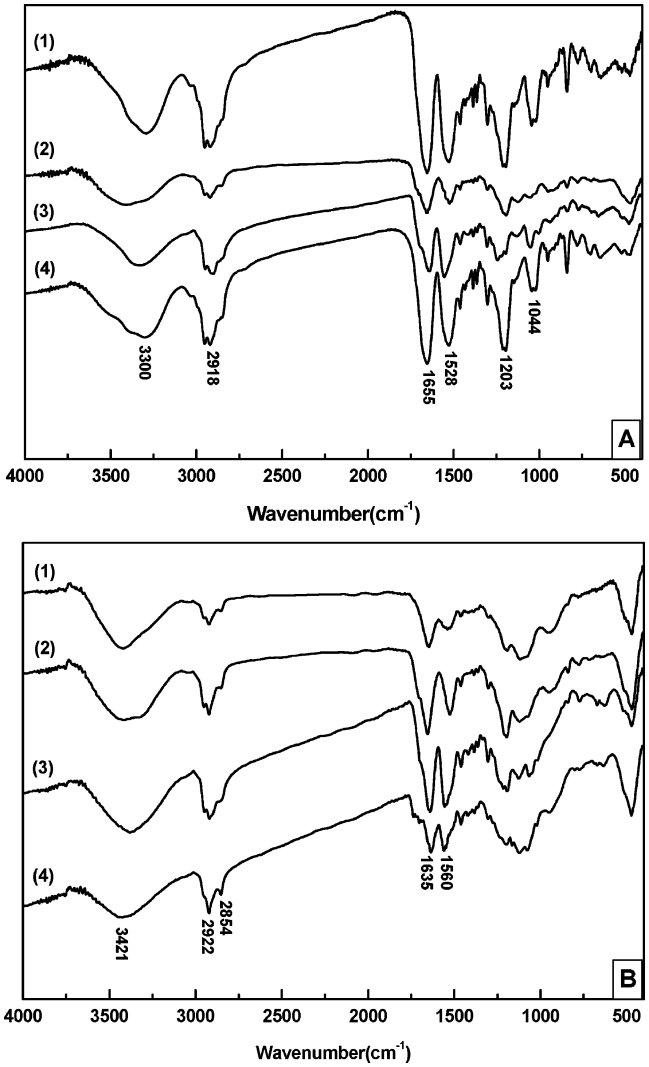

Figure 6. FTIR spectra of precursors/PTU composite films before (A) and after (B) reaction with H_2S: (1) 22.8 wt % precursors; (2) 26.3 wt % precursors; (3) 51.2 wt % precursors; (4) 59.3 wt % precursors.

polymer networks. After treatment of the precursors/PTU composite films with H_2S (Figure 7b), the maximum absorption peak at 357 nm of precursors/PTU composites disappears and the typical absorption curves of PbS nanoparticles appear in the spectra, confirming the formation of PbS nanoparticles in polymer matrix in situ after exposure to H_2S gas.

Figure 6 shows the IR spectra of precursors/PTU composites with various precursor contents before and after treatment with H_2S. After reaction of precursors with PTU oligomer, the absorption peaks at 2268 cm^{-1} for isocyanate groups disappear. Although the precursor (22.8 wt %)/PTU film sample (1) has excess isocyanate groups of PTU oligomer compared with hydroxyl group of precursors, the absorption peak of isocyanate groups cannot be observed in FTIR spectra. The reason may be that the excess isocyanate groups react with moisture in air or self-polymerize. The characteristic vibrations of O−H bonds for precursors and N−H of thiourethane linkages for PTU appear at 3300 cm^{-1}, and the absorption bands gradually become broader and shift to longer wavenumber with increasing content of precursors, indicating that the content of hydroxyl groups is increasing. At the same time, the peaks at 1044 cm^{-1}, which are assigned

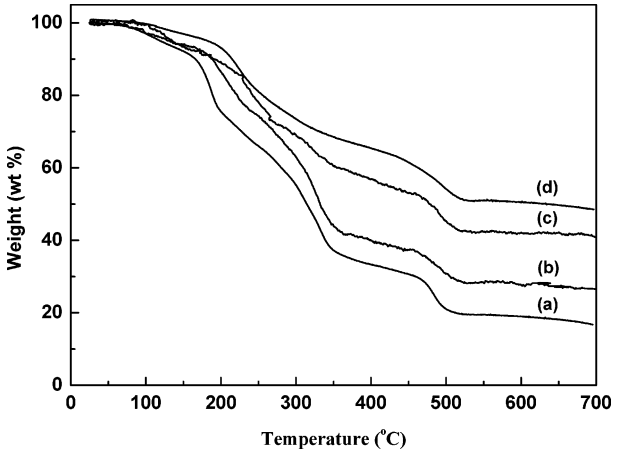

Figure 7. TGA curves of precursors/PTU composite films after treatment with H_2S: (a) 22.8 wt %; (b) 26.3 wt %; (c) 51.2 wt %; (d) 59.3 wt % precursors.

Table 2. Properties of the PbS/PTU Nanocomposite Films

Pb−PTU[a]	PbS−PTU[b]	n_d (632.8 nm)[c]	n_d (632.8 nm)[d]	700 °C residue[e]
0	0	1.574	1.574	
11.9	7.80	1.579	1.612	
22.8	14.8	1.595	1.664	16.8
26.3	17.0	1.600	1.680	26.6
37.0	23.7	1.616	1.707	
42.3	27.0	1.624	1.762	
51.2	32.4	1.633	1.812	41.2
59.3	37.3	1.646	1.872	48.6
66.9	41.8	1.665	2.055	

[a] Weight content of precursors in the composite films before treatment with H_2S gas. [b] PbS content in the PbS/PTU nanocomposite films. [c] Refractive index of the composite films before treatment with H_2S gas. [d] Refractive index of the PbS/PTU nanocomposite films. [e] Char yield of the nanocomposite films after TGA at 700 °C.

to the characteristic vibrations of C−O bond for precursors, also increase in intensity with increasing content of precursors, compared with the intensity of characteristic absorption bands of benzene ring at 1528 cm^{-1}. After exposure of the precursors/PTU films to H_2S gas, the absorption peaks at 3300 cm^{-1} sequentially shift to longer wavenumber, compared with that before treatment with H_2S gas. The probable explanation is that the coordination effect of hydroxyl groups with lead ions or hydrogen bond between hydroxyl groups become weaker in the nanocomposite systems. Another possible reason is that the formation of PbS particles in polymers destroyed self-hydrogen bonding between hydroxyl groups.

Figure 7 illustrates TGA curves of precursors/PTU composite films with various contents of precursors after reaction with H_2S. The residues of the nanocomposite films at 700 °C are in the range of 17−50 wt % and they increase with increasing precursor content in the films. As shown in Table 2, the residues of 16.8, 26.6, 41.2, and 48.6 wt % for the composite films with different contents of precursors at 700 °C are higher than that of the theoretical content of inorganic phase PbS, particularly, in the composite films with high content of precursors. This reason may be that the covalent linkages between organic and inorganic phase trapped the organic moiety in the inorganic phase or residual carbons after high-temperature calcination.[19] This case also occurred in the TGA characterization of lead-containing precursors.

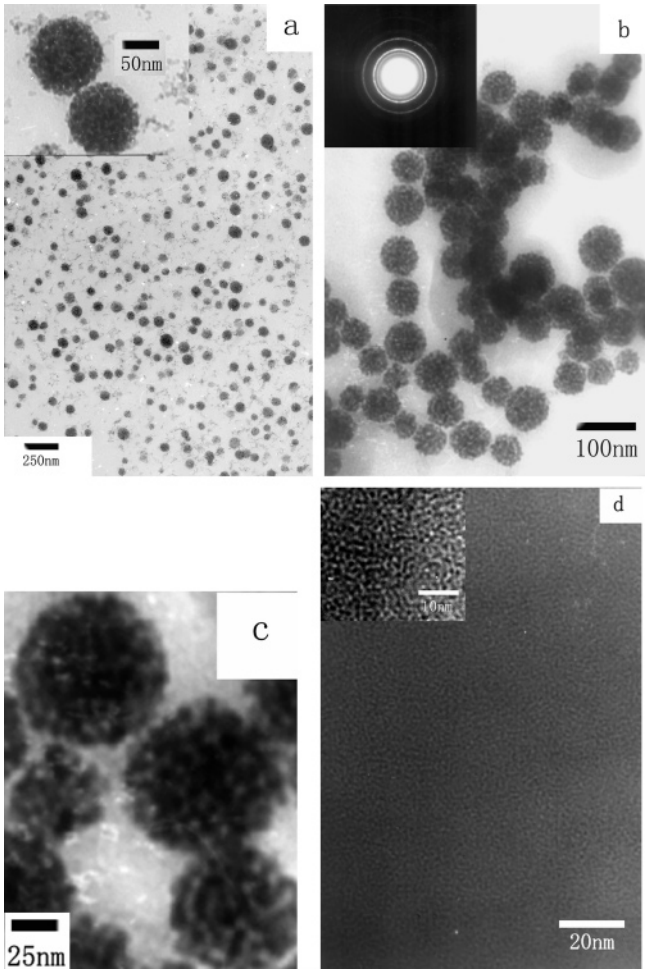

Figure 8. TEM images of PbS/PTU nanocomposite films obtained from the precursor content of (a) 26.3 wt % based on microtome method; (b) 26.3 wt % deposited on the carbon grid; (c) higher magnification picture for (b); (d) 59.3 wt % obtained from microtome method.

Figure 8a−c and Figure 8d show the TEM micrographs of PbS/PTU nanocomposite films obtained from 26.3 wt % and 59.3 wt % precursors, respectively. Figures 8a and 8b are the TEM images under different preparation conditions of samples. The TEM image in Figure 8a was prepared by ultracut microtome and that in Figure 8b was prepared by casting a drop of suspension solution of ethanol containing nanocomposite powders on a carbon-coated copper grid after ultrasonic treatment. Figure 8c is the higher magnification picture of Figure 8b. It can be clearly seen that the size of PbS nanoparticles formed in situ in polymer networks are below 10 nm without larger aggregation for both low and high content of precursors, although many nanospheres are observed for nanocomposite samples obtained from low content of precursors. However, the PbS particles formed in DMSO from precursors using gas/liquid reaction exhibit larger aggregation phenomenon. These results indicate that the polymer plays an important role in controlling the size and monodispersion of PbS nanoparticles because the polymer networks obtained from lead-containing precursors and PTU oligomer with isocyanate groups have large numbers of thiol end groups that strongly bond to the particles surface, which can effectively prevent the particles from growing and aggregating further after nucleation.

In addition, we can also find from TEM images that the dispersion form of PbS nanoparticles formed in polymer matrix is obviously different. Many spherical aggregates that ranged from 50 to 100 nm are uniformly dispersed inside the nanocomposite films obtained from low precursor content (26.3 wt %) (Figures 8a and 8b). From the amplificatory photograph (inset of Figure 8a and Figure 8c), it can be seen that these spherical aggregates are clearly composed of individual PbS nanoparticles as a discrete entity below 10 nm and there a small quantity of dispersive nanoparticles with the same size exists outside the nanospheres. However, for the nanocomposite sample obtained from high precursor content (59.3 wt %), the PbS nanoparticles of about 3 nm disperse uniformly in the whole polymer matrix and display a narrow distribution in size (Figure 8d).

We think that the ratio of lead-containing precursors to oligomer may be a primary reason affecting the phase behavior of PbS/polymer nanocomposites. As the precursor content is below 26.3 wt %, the hydroxyl groups have completely reacted with isocyanate groups at stoichiometric amounts. The PTU oligomer with short molecule chains, as cross-linking reagent, reacts with the precursors, which may result in a domain rich in lead ions. Especially for the nanocomposite film obtained from 26.3 wt % precursors, the degree of cross-linking reaction between precursor and PTU oligomer reaches maximum value. After reaction with H_2S, the formed PbS nanoparticles are mostly confined within the domain rich in lead ions. In addition, to minimize surface free energy, the domains presented nanospherical shape on the whole. This case also occurred in another PbS/polymer composite system.[37] When the content of precursor in the composites is higher, the cross-linking reaction between PTU oligomer and precursors obviously decreases because the hydroxyl groups on precursors are in excess compared with isocyanate groups of PTU oligomer. As a result, the lead-containing precursors do not aggregate together by a cross-linking reaction, the larger domains rich in lead ions cannot be produced, and the lead ions relatively uniformly distribute within the polymer networks. After exposing the films to H_2S gas, the formed PbS nanoparticles uniformly disperse in the whole polymer matrix. In the experiment, we found that before forming films, the mixture solution of PTU oligomers and low content of precursors were prone to produce precipitates after 12 h, indicating that the obviously cross-linking reaction between precursors and oligomers occurred, and the formed larger aggregates as precipitates separated from the solution. However, this case did not appear for the mixture solution with high content of precursors (>26.3 wt %). This phenomenon also indirectly demonstrates that the content of lead-containing precursors has an important effect on the phase behavior of nanocomposites. Further studies on the phase behavior of the nanocomposite and the factors affecting domain size can test this hypothesis proposed above and provide the detailed mechanism.

Figure 8b (inset) is the selected area electron diffraction pattern (SAED) for the 17 wt % of PbS/PTU nanocomposite

(37) Gao, M. Y. Assembly of Nanoparticles in Polymer Matrices and Ultrathin Film. Ph.D. Thesis, Jilin University, 1995; Chaper 2.

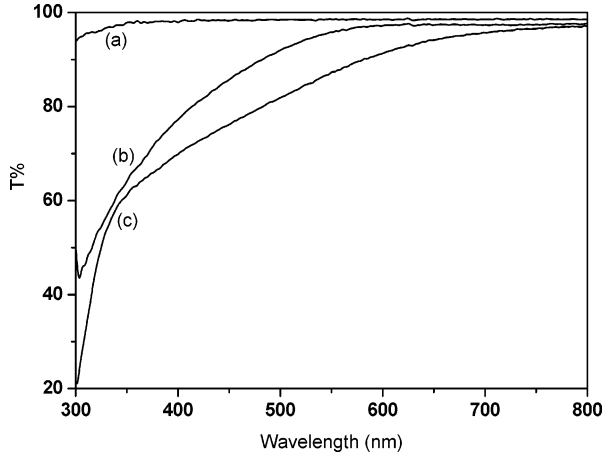

Figure 9. Uv−vis transmittance spectra of PTU polymer (a) and PbS/PTU nanocomposite thin films with PbS contents of 17 wt % (b) and 37 wt % (c).

film. The SAED pattern exhibits broad diffuse rings with (111), (200), (220), (311), (222), (400), (420), and (422) planes, which is in agreement with the cubic phase of PbS.

Optical transparency of the PbS/PTU nanocomposite thin films with a thickness of about 1 μm on the glass plates, using a blank glass plate as the reference, was characterized by UV−vis spectra. The results indicate that the pure polymer matrix (PTU) has high transmittance (>98%) at 350−800 nm and all the nanocomposite films containing PbS particles exhibit good transparency (>90%) above 600 nm, although the PbS particles have strong absorption below 600 nm in the UV−vis region. Usually, the transparency of nanocomposite films with PbS nanoparticles is mainly dependent on the size and content of PbS particles. Figure 9 shows the UV−vis transmittance spectra of polymer matrix (PTU) and nanocomposite thin films with PbS content of 17 wt % and 37.3 wt %, respectively.

For the PbS/PTU nanocomposite system, when the content of lead-containing precursors is above 67 wt %, the resulting nanocomposite films with good mechanical properties cannot be obtained. So here we only prepared the nanocomposite films obtained from the lead-containing precursors below 67 wt %. The refractive indices of the composite films before (precursors/PTU) and after (PbS/PTU nanocomposite) treatment with H_2S gas were measured at 632.8 nm by an ellipsometer. The refractive index variation of the composite films with the weight content of the lead-containing precursors is shown in Figure 10. The refractive index of precursors/PTU composite films increases from 1.574 to 1.665 with the weight content of the lead-containing precursors from 0 to 67 wt %. It is obvious that the lead-containing precursors have a great contribution to the increase of refractive index for polymer composites. After treatment of the precursor/PTU composite films with H_2S gas, the refractive index of the obtained PbS/PTU nanocomposite films again obviously increases, indicating that the formed PbS particles have a greater contribution to the increase of the refractive index compared with the lead-containing precursors (Table 2). For the nanocomposite obtained from 67 wt % of precursor, the

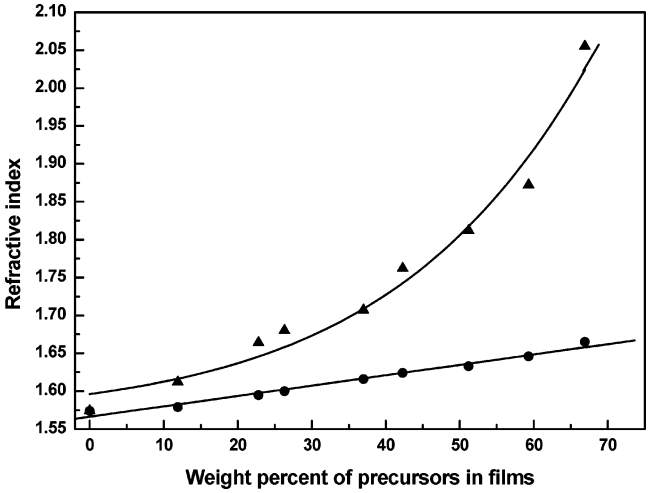

Figure 10. Refractive index change for precursors/PTU composite films and PbS/PTU nanocomposite films with weight content of the precursors in films.

refractive index has reached 2.055 (Table 2). From Figure 10, it can also be seen that the refractive index of precursors/PTU composite films linearly increases with the weight content of the lead-containing precursors. However, there is no linear dependence of the refractive index of PbS/PTU nanocomposite films on the precursor weight fraction. The refractive indices of pure precursors and PbS/ME complexes were calculated to be about 1.725 and 2.8 by regression analysis, respectively.

Conclusions

In summary, a series of PbS/PTU nanocomposite films with high refractive index have been successfully prepared from composites with a linkage of lead-containing precursors through in situ gas/solid reaction. The morphology studies suggest that the formed PbS nanoparticles in polymer networks display different dispersion fashion; however, the size of the PbS nanoparticles is below 10 nm. These results inspire us to explore the phase behavior of the different nanocomposites which can be obtained from different metal-containing precursors, including different organic ligands with double bond or hydroxyl groups and different metal ions, such as lead, zinc, and cadmium ions as well as different polymer networks including oligomer capped with reactive functional groups or macromolecules with reactive functional groups on the side chains. The present method provides a novel route for fabricating high refractive index nanocomposite films, which enables us to incorporate the high content of PbS nanoparticles into oil-soluble polymer matrix via chemical bonding and can better extend the potential application of these nanocomposites in many fields, especially in high refractive index optical coatings.

Acknowledgment. This work was supported by the Special Funds for High Tech Research and Development Project (No. 2002AA302612, No. 51412020103JW1302) and Young Science Foundation of NE Normal University (No. 111494015).

CM050113N